From a Bird's Eye View to See: Joint Camera and Subject Registration without the Camera Calibration

Zekun Qian¹, Ruize Han¹, Wei Feng¹, Feifan Wang¹, Song Wang²

¹ College of Intelligence and Computing, Tianjin University, Tianjin, China

² Department of Computer Science and Engineering, University of South Carolina, USA

{clarkqian, han_ruize, wfeng, wff}@tju.edu.cn, songwang@cec.sc.edu

Abstract

We tackle a new problem of multi-view camera and subject registration in the bird's eye view (BEV) without pregiven camera calibration. This is a very challenging problem since its only input is several RGB images from different first-person views (FPVs) for a multi-person scene, without the BEV image and the calibration of the FPVs, while the output is a unified plane with the localization and orientation of both the subjects and cameras in a BEV. We propose an end-to-end framework solving this problem, whose main idea can be divided into following parts: i) creating a viewtransform subject detection module to transform the FPV to a virtual BEV including localization and orientation of each pedestrian, ii) deriving a geometric transformation based method to estimate camera localization and view direction, i.e., the camera registration in a unified BEV, iii) making use of spatial and appearance information to aggregate the subjects into the unified BEV. We collect a new large-scale synthetic dataset with rich annotations for evaluation. The experimental results show the remarkable effectiveness of our proposed method.

1. Introduction

There are just three problems in computer vision: registration, registration, and registration.

- Takeo Kanade

Registration is an important task in computer vision. In this work, we study a new and challenging problem of *camera and person* (referred to as subjects in this paper) *registration in the BEV without camera calibration*. Specifically, as shown in Figure 1, given the multi-view images for a multi-person scene, we aim to achieve both the camera and subject registration in the bird's eye view, where the camera registration denotes the camera localization and view direction estimation, and the subject registration denotes the subject localization and face orientation estimation. Note that,

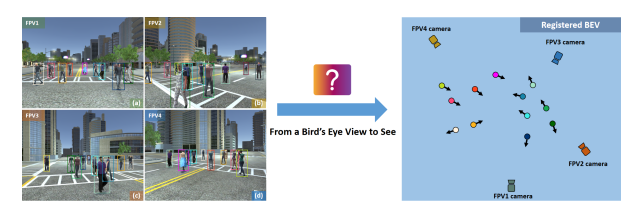


Figure 1. An illustration of the multi-view camera and human registration problem.

in this work, we register the subjects in the BEV but without a real bird's-eye-view image, where we generate a virtual BEV. Moreover, we do not use the camera calibration as input (in previous works), but we need generate a camera registration result, i.e., the camera location and view direction estimation (can be regarded as a weak version of the camera calibration) as output.

The proposed problem is practical for the multi-view camera multi-human scene analysis, which has many applications such as video surveillance, social scene understanding, etc. In this case, the bird's eye view, also called as top view, is a good way for observing the whole scene. In BEV, we can obtain the global spatial layout and trajectories of all the persons in the scene without mutual occlusion, which has some typical scenarios including the automatic driving [11,28,29,31,41], outdoor human detection [4,10] and complementary-view crowd analysis [14,18].

A popular research problem related to this task is the multi-view human detection [4, 10, 22, 23, 38], which projects the subjects detected from each view to their locations on the ground plane, and then generate an occupancy map in the bird's eye view. Note that, these methods all *require the pre-given camera calibration parameters* among the multi-view cameras as input, which, however, limits the applications of the method in many scenes. Another series of research focus on the complementary-view multi-human analysis using a top-view camera (e.g., on a UAV) and several first-person-view cameras [14, 15, 17, 18]. The main limitation of these methods is that the usage of *a top-view camera carried by a drone is not easy to deploy*.

The proposed problem is very difficult given the *very* limited input information and multiple output results. In this paper, we propose a new framework for this problem, in which we simultaneously achieve two tasks of 1) subject detection and fusion, 2) camera localization and view direction estimation, in the BEV. We clarify that these two tasks can complement each other and be jointly solved in a unified framework. Specifically, in each view, we first apply a view-transform subject detection module (VTM) to obtain the subject detection results in the BEV. Meanwhile, we use a multi-view human association module to obtain the cross-view human consistency among the multiple views. With the human detections with identification consistency, we propose a computing geometry based spatial alignment module (SAM) to estimate the relative pose between the cameras in the BEV (camera registration). With the camera registration, we can get unified subject detection (subject registration) in the BEV. We summarize the main contributions in this work:

- We systematically study the camera and subject registration problem for the multi-view multi-human scene analysis, including the problems of camera localization, view direction estimation and human registration in a unified BEV. This work breaks the limitations in previous works that require the pre-given camera calibration or real BEV image.
- **②** We propose a preliminary solution for this problem, in which we integrate the deep network based human detection and association module and a multi-view geometry based camera pose estimation module. This framework integrates both the generalization of the deep network for the human identification task and the stability of the classical geometry for camera pose estimation task.
- **19** We build a new large-scale synthetic dataset for the proposed problem. Extensive experimental results on this dataset show the superiority of the proposed method and the effectiveness of the key modules. Also, the real case study verifies the generalization of our framework.

2. Related Work

Multi-view object detection. The most related work to this paper seems to be multi-view object detection, which aims to aggregate information of the same object from different views. The main difficulty of this problem is solving the serious occlusion problem. Recent approaches for this work are mainly based on the pre-given camera calibration parameters to project the object detected from each view to their locations on the real-world ground plane, and then generate an occupancy map in the bird's eye view (BEV). In [4, 10], researchers estimate the positions of pedestrians on the ground plane with corresponding anchor box features. In [22, 23, 38], feature perspective transformation is employed to project all view features into a shared plane without any anchor. A couple of datasets for multi-view

pedestrian detection, one built in a virtual environment and one captured from the real world, are proposed in [9, 23], respectively. Besides the multi-view detection, some recent related works have been employed in different fields, e.g., cross-view human association and tracking, multi-view 3D human pose estimation [12, 35, 40], etc. Note that, these works all use fixed cameras and require the prior camera calibration parameters as input. Differently, in this work, we do not need the pre-given camera calibration parameters and also provide the camera registration results in the BEV as output.

Monocular RGB image 3D object detection. Monocular RGB 3D object detection aims to estimate the 3D position of objects from monocular images without the information from depth sensors. One of the hottest applications is autonomous driving, in which recorded videos involving lots of pedestrians and cars to be detected. For this problem, previous works [5, 6, 11, 21, 28, 29, 41] propose some outstanding structures of network with some special designs, such as non-local attention block, depth-conditioned dynamic message propagation and so on. For example, in [5], a lightweight network is employed to predict the depth of each pedestrian by skeletons and estimate the uncertainty of the result. Based on [5], a new network structure is proposed in [6], which can be used to not only predict the 3D localization but also can estimate the orientation of each object. Differently, in this work, we are more interested in the pedestrian (and camera) 3D localization from the multiview cameras, the collaborative analysis of which can provide more information than the monocular camera and has many practical real-world applications, e.g., video surveillance in open scenarios.

Camera pose estimation. A related problem to this work is camera pose estimation, which is a fundamental problem in computer vision. In the long history of its exploration, many methods have been proposed. Conventional methods to solve this problem used to be helped with some extra measuring devices. In [26], the laser rangefinders are used to combine cameras from different views. In [7, 13], the visual sensors are applied to bridge the huge differences between different field of views (FOV). In [8, 34], some structure from motion (SfM) methods are proposed to track the movement of objects from different views. The core for recent vision based methods [20, 33] is to find and match the feature points from different views, which, however, are not very useful in this work given the large FOV difference.

Bird's-eye-view visual analysis. Recently, some works propose to associate the top view (bird's eye view) with the first-person views for collaborative analysis. In [36, 37], such idea is employed to locate the first-person-view camera in BEV aerial images in a large field, which is used for GEO-localization. Later, some related works [14,15,17,18] focus on the localization of humans, which aims to asso-

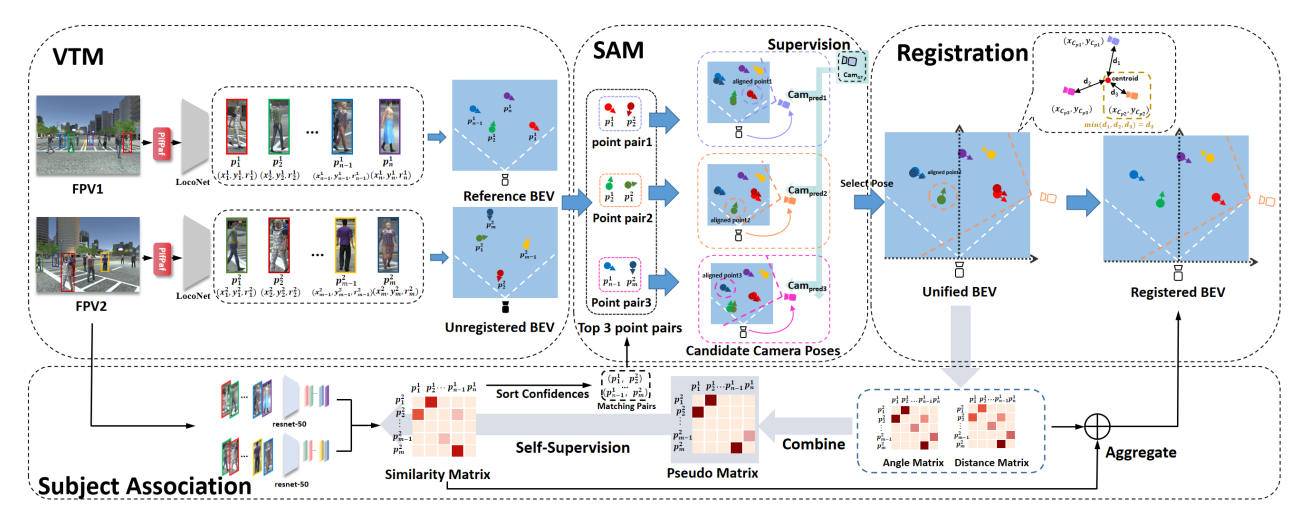


Figure 2. Framework of the proposed method, which can be divided into four parts, i.e., VTM, SAM, Registration and Subject Association. We use a hollow camera graph to represent a registered camera and a filled camera pattern to represent an unregistered camera.

ciate and track the multiple humans by the spatial reasoning based on the pre-acquired detection. Another series of related works [1–3] use graph matching based methods to locate camera wearers by combining information from FPVs and BEV. The main difference between the previous works and this work is that they require a BEV image (e.g., captured by a UAV) as input, which is not very practical in many real-world applications.

3. Proposed Method

3.1. Overview

We first give an overview of the proposed method mainly containing three stages, as shown in Figure 2. 1) Given multiple images simultaneously captured from different views for a multi-human scene, we apply a view-transform subject detection module (VTM) to get the position and the face orientation estimation of each person in the BEV. We then apply a multi-view human association module to select the matched subjects, with which a geometric transformation based spatial alignment module (SAM) is used to estimate the relative camera pose candidates in the BEV (Section 3.2). 2) We next use a centroid distance based candidate selection strategy to choose the final camera pose estimation result (camera registration) from the candidates obtained by the SAM. For the subject registration task, we take both spatial and appearance information to aggregate the same person in the BEV for multi-view person localization fusion (Section 3.3). Finally, with the subject registration results, we propose a backward training strategy to learn subject similarity in the human association module in a self-supervised manner. (Section 3.4).

3.2. Cross-view Camera Pose Estimation

View-Transform Subject Detection Module (VTM).

For the input of multiple images capturing a multi-human scene, we first get the subject position and face orientation of each person in the BEV. For this purpose, we develop a **LocoNet** using a lightweight FC-based structure with three heads. Before that, we first apply an existing human pose



Figure 3. The structure of LocoNet. Here $\times 512$ means the layer outputs 512 feature channels, Fc means fully connected layer, BN means batch normalization layer, ReLU is an activation function, DP0.2 is the dropout layer with ratio 0.2.

detector called PifPaf [25] to predict the 2D skeleton joints of each person from the original RGB image, which can be regarded as a low-level representation of each person. The skeleton joints are inputted into the LocoNet, whose structure is shown in Figure 3. At the end of LocoNet, we use a human 3D localization head composed of simple MLP layers to predict the position and face orientation of each person. The process of the network can be represented as

$$\mathbf{p}_{i}^{v} \triangleq (x_{i}^{v}, y_{i}^{v}, r_{i}^{v}) = \text{LocoNet}(\mathbf{k}_{i}^{v}), \tag{1}$$

where v denotes the v-th view and i denotes the i-th person in v-th view, \mathbf{k}_i^v is the 2D skeleton joints belonging to the person i in view v. \mathbf{p}_i^v is the output prediction of LocoNet, which is composed of (x_i^v, y_i^v) representing the subject position in the BEV and r_i^v representing the face orientation.

Spatial Alignment Module (SAM). We then show the relative camera pose estimation (in the BEV) via the subject localization alignment. For convenience, we first present

the relative camera pose estimation between two views. Our basic idea is that the human position and face orientation are unique in the real-world 3D coordinate system, which is various in the multiple 2D images taken by different cameras. In the BEV maps with human position and face orientation generated from different first-person view (FPV) images, we can obtain the camera pose in the BEV by aligning the corresponding human position and facing orientation as shown in SAM of Figure 2.

For this purpose, the first step is to find the same subject from different views. We identify the subjects in the input images through the human appearance features, and the corresponding subjects in the BEV are then matched across different views. We use a CNN network to extract the feature of every person and apply Euclidean distance and sigmoid function to create a similarity matrix (\mathbf{M}_{pred}), which indicates the subject similarities among the subjects from two views. Then we sort the similarities of each matching pair and select the top-K pairs as the *matching pairs*.

After that, we apply the geometric transformation to align two BEVs (containing all subjects and the camera on them), which are denoted as a reference BEV map and an unregistered one. Specifically, for a pair of associated points, we apply a geometric transformation, as shown in Figure 4, to rotate and move the camera position and orientation in the unregistered BEV to that in the reference BEV.

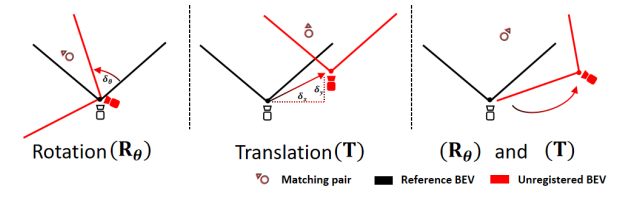


Figure 4. An illustration of the rotation and translation transformation for two BEVs with a matching pair.

We calculate the relative pose (in the BEV) between two points in a matching pair as discussed above, which are denoted as $\mathbf{p}_{\rm ref}=(x_{\rm ref},y_{\rm ref},r_{\rm ref})$ and $\mathbf{p}_{\rm unr}=(x_{\rm unr},y_{\rm unr},r_{\rm unr})$. Specifically, the relative pose transformation between them can be formulated as

$$\begin{pmatrix} x_{\text{ref}} \\ y_{\text{ref}} \\ 1 \end{pmatrix} = \mathbf{TR}_{\theta} \begin{pmatrix} x_{\text{unr}} \\ y_{\text{unr}} \\ 1 \end{pmatrix}, \tag{2}$$

where
$$\mathbf{R}_{\theta} = \begin{pmatrix} \cos \delta_{\theta} & -\sin \delta_{\theta} & 0 \\ \sin \delta_{\theta} & \cos \delta_{\theta} & 0 \\ 0 & 0 & 1 \end{pmatrix}$$
, $\mathbf{T} = \begin{pmatrix} 1 & 0 & \delta_{x} \\ 0 & 1 & \delta_{y} \\ 0 & 0 & 1 \end{pmatrix}$.

We denote \mathbf{R}_{θ} as the rotation matrix with a rotation angle δ_{θ} , and \mathbf{T} is the translation matrix, in which (δ_x, δ_y) is the translation vector.

The corresponding matching pair can be aligned after applying this transformation. This means the transformation

matrix is just the relative camera pose between the two cameras in the BEV. Note that, this relative camera pose only contains three degrees of freedom, i.e., the translation and rotation projected into the BEV plane. This way, we can obtain the relative camera pose $(\delta_x, \delta_y, \delta_\theta)$ by solving the above Eq. (2) and get

$$\begin{cases} \delta_x = x_{\text{ref}} - x_{\text{unr}} \cos \delta_{\theta} + y_{\text{unr}} \sin \delta_{\theta} \\ \delta_y = y_{\text{ref}} - x_{\text{unr}} \sin \delta_{\theta} - y_{\text{unr}} \cos \delta_{\theta} \\ \delta_{\theta} = r_{\text{ref}} - r_{\text{unr}} \end{cases}$$
(3)

As discussed above, we use K point pairs to estimate the relative pose, each of which can generate a relative pose estimation result as it is shown in SAM in Figure 2. We use the camera pose estimation loss function for training as

$$\mathcal{L}_{\text{Cam}} = \sum_{i=1}^{K} (\|(\delta_x^k, \delta_y^k) - (\delta_x^{\text{gt}}, \delta_y^{\text{gt}})\| + \|\delta_{\theta}^k - \delta_{\theta}^{\text{gt}}\|), \quad (4)$$

where $(\delta_x^k, \delta_y^k, \delta_\theta^k)$ is the k-th candidate relative camera pose estimation generated from the k-th point pair, and $(\delta_x^{\rm gt}, \delta_y^{\rm gt}, \delta_\theta^{\rm gt})$ is the ground-truth camera pose. Note that, we apply the supervision on the camera position, i.e., δ_x, δ_y , and the view orientation, i.e., δ_θ in our method. However, the camera view direction is very hard to measure and annotate in real-world applications. In the experiments, we show that our method is not very sensitive to the supervision of δ_θ .

3.3. Camera and Subject Registration

Camera registration. Based on the relative camera pose $(\delta_x^k, \delta_y^k, \delta_\theta^k)$ obtained in Section 3.2, we have got K candidates of relative camera pose estimation between the reference and unregistered BEVs. Here we denote the camera pose on the reference BEV as (0, 0, 0). We then get a camera pose of the unregistered BEV on the coordinate system of the reference BEV as

$$\mathbf{c}^{k} = (c_{x}^{k}, c_{y}^{k}, c_{\theta}^{k}) = (0, 0, 0) + (\delta_{x}^{k}, \delta_{y}^{k}, \delta_{\theta}^{k}) = (\delta_{x}^{k}, \delta_{y}^{k}, \delta_{\theta}^{k}),$$
(5)

which denotes the k-th candidate camera pose from $(\delta_x^k, \delta_y^k, \delta_\theta^k)$, as shown in Figure 5.

The next step is to find the selected camera pose from the K candidates, i.e., achieving the camera registration task. $\overline{c_x} = \frac{\sum_{k=1}^K c_x^k}{K}, \overline{c_y} = \frac{\sum_{k=1}^K c_y^k}{K}, \text{ where } (c_x^k, c_y^k) \text{ is the candidate position of the unregistered camera, } (\overline{c_x}, \overline{c_y}) \text{ is the centroid point. We then compute the distance of each candidate position to the centroid point as}$

$$d_{\text{centroid}}^k = \|(c_x^k, c_y^k) - (\overline{c_x}, \overline{c_y})\|, \tag{6}$$

The candidate with the minimum distance will be selected, which is used to register the unregistered BEV into the reference BEV, then we can get a unified BEV as shown in the left part of Registration in Figure 2.

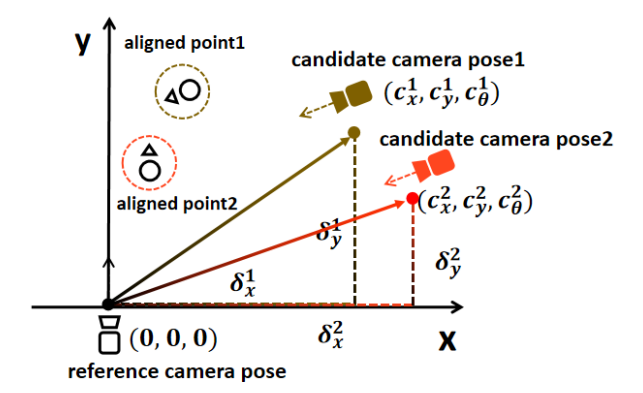


Figure 5. Candidate camera poses in the coordinate system.

Subject localization fusion. With the camera registration result, we can register the camera position and its view direction, together with the subject localization and face orientation of the unregistered BEV, into the reference BEV. Note that, for multiple views, we select one as the reference BEV and others as the unregistered BEVs, all of which can be registered into the reference BEV, respectively. The next step is aggregating the same person from different views in the unified BEV, which can be achieved by two steps, i.e., subject matching and fusion.

1) Subject Matching. To match the subjects from multiple views, we create a person spatial distance matrix $\mathbf{M}_{\mathrm{dis}}$ and an angle difference matrix $\mathbf{M}_{\mathrm{ang}}$ in the unified BEV, which measure the distance and angle differences of all persons from different views. We then combine it with similarity matrix $\mathbf{M}_{\mathrm{pred}}$ provided in Section 3.2. We first use three thresholds as masks to preliminarily select matching pairs, in which only the pair satisfying all three conditions will be regarded as the same person. Besides, we further consider two constraints for accurate matching. The first one is cycle consistency [24], which means the connection of the same subject from all views should form a loop. The second one is uniqueness, which means one subject should not be connected to more than one subject in another view.

First, we use a classical data structure, i.e., union-find, to aggregate the transitive relations, which makes all the subjects with direct and indirect connections in a union of union-find to be clustered as a sub-graph, as shown in Figure 6(b), which solves the problem of cycle consistency for all the subject connected as a loop. Second, we define the problem as a hierarchical maximum spanning subgraph problem, the layer-by-layer (view-by-view) spanning constrain that a subject is connected at most one node in each view to avoid the uniqueness conflict, as shown in Figure 6(c). To solve this problem, we propose an algorithm referenced from the Prim algorithm [30]. We provide more details and the algorithm flow of the above strategy in the supplementary material.

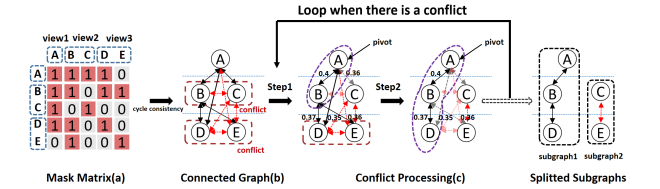


Figure 6. Example of the cycle consistency and uniqueness.

2) Subject Fusion. For the subjects from multiple views to be regarded as the same person using the above subject matching method, we then estimate the final position of it using the same strategy in Eq. (6). The subject position with the minimum centroid distance will be retained and other points will be removed. Especially, if there are only two views, we use the mean value of two points as the fused one. Finally, we can get the unified BEV with the camera and subject registration from multiple different views.

3.4. Self-supervision for Subject Association

Based on the above subject registration results, we further consider to backward supervise the appearance based subject association. As shown in the bottom of Figure 2, we propose to train the appearance feature extraction network for similarity matrix calculating in a self-supervised manner, to make full use of the spatial information from Section 3.3. Specifically, we inversely normalize each row of the spatial distance matrix \mathbf{M}_{dis} and angle difference matrix \mathbf{M}_{ang} discussed above, to get the spatial-aware similarity matrixes as $\mathbf{M}_{\text{spatial}} = \alpha \overline{\mathbf{M}}_{\text{dis}} + (1-\alpha) \overline{\mathbf{M}}_{\text{ang}}$, where α is the hyper-parameter, $\overline{\mathbf{M}}_{\text{dis}}$ and the $\overline{\mathbf{M}}_{\text{ang}}$ are the normalized similarity matrix obtained from \mathbf{M}_{dis} and \mathbf{M}_{ang} , respectively. After that, we apply a self-supervised loss to train the appearance feature extraction network as below

$$\mathcal{L}_{\mathrm{App}} = \|\mathbf{M}_{\mathrm{pred}} - \mathbf{M}_{\mathrm{spatial}}\|. \tag{7}$$

3.5. Implementation Details

We pretrain the LocoNet using the location and orientation labels in our synthetic data with MSE loss and use the pretrained model of ResNet-50 in [16]. We use the camera pose loss function and the self-supervised appearance learning loss function as the total loss function $\mathcal{L} = \mathcal{L}_{\text{Cam}} + \mathcal{L}_{\text{App}}$. We set the number of candidate K as 3 in Section 3.2 and the similarity matrix threshold as 0.25, distance threshold as 2.0 m and angle threshold as 15° in Section 3.3. We set the hyper-parameters of the pseudo matrix in Section 3.4 as $\alpha = 0.5$. We use a pair of FPVs to train our framework. In the inference stage, the number of FPVs is not limited, in which one FPV will be selected as the reference view and others can be registered in that reference view. We use Pytorch as our main framework and the work runs on the server with RTX 3090 GPU.

Table 1. Camera registration results. The top half is comparison experiments, the bottom half is ablation experiments and the last row is the result of our proposed method, in which 'Cam.Pos.Avg' and 'Cam.Ori.Avg' present the average error in meters of the camera position and the orientation error in degrees in BEV, 'Cam.Pos@d' represents the percentage of distance error within d meters and 'Cam.Ori.@r' represents the percentage of angle error within r degrees.

	Cam.Pos.Avg	Cam.Ori.Avg	Cam.Pos@0.5	Cam.Pos.@1	Cam.Pos.@1.5	Cam.Ori.@5	Cam.Ori.@10	Cam.Ori.@15
Monoloco++ [6]	3.00	21.84	7.60%	21.60%	36.40%	17.50%	34.60%	47.10%
DMHA [15]	5.99	47.43	46.50%	47.60%	48.60%	46.20%	50.00%	53.60%
SIFT [27]	7.11	144.46	1.26%	2.34%	3.60%	4.80%	8.20%	11.10%
Matching [20]	11.84	92.04	0.51%	0.82%	1.33%	3.70%	6.50%	8.50%
Max	2.27	15.22	20.00%	42.30%	59.60%	33.90%	60.30%	76.00%
Random	1.91	12.62	21.60%	47.30%	65.00%	37.50%	65.80%	81.20%
w/o pre-train	6.98	33.02	0.50%	1.40%	3.20%	10.20%	20.90%	29.50%
w/o GT δ_{θ}	0.93	5.91	37.80%	71.80%	85.60%	59.10%	85.60%	94.30%
Ours	0.89	5.78	42.20%	72.40%	88.40%	59.50%	86.50%	94.80%

Table 2. Subject registration results. The expression of metrics of subject here is in the same way as Table 1.

	Sub.Pos.Avg	Sub.Ori.Avg	Sub.Pos.@0.5	Sub.Pos.@1	Sub.Pos.@1.5	Sub.Ori.@5	Sub.Ori.@10	Sub.Ori.@15
Monoloco++ [6]	1.32	32.50	26.05%	61.47%	77.65%	13.21%	26.05%	38.17%
MVDetr [22]	2.41	-	11.18%	29.54%	46.07%	-	-	-
MVDet [23]	2.44	-	11.28%	29.19%	45.65%	-	-	-
Max	1.27	21.56	37.39%	72.38%	82.87%	30.46%	54.95%	69.13%
Random	1.06	17.19	39.19%	74.62%	85.07%	33.61%	59.01%	73.39%
w/o pre-train	6.35	89.29	1.62%	6.62%	11.41%	2.29%	4.74%	6.97%
w/o GT $\delta_{ heta}$	0.83	16.36	41.15%	77.89%	89.31%	32.30%	56.79%	72.77%
Ours	0.75	14.67	43.23%	81.43%	92.12%	35.07%	63.24%	79.15%

4. Experiments

4.1. Dataset

Synthetic dataset. To our best knowledge, there are no available datasets that can be used for the task in this work, which requires the multi-view relative camera poses, the 3D position and the face orientation of each person. Even with expensive hardware, it is also very hard to obtain accurate annotations of them in the real world. So we consider using the modeling engine to create a synthetic dataset.

- Flexible data controlling. We use a 3D game development Unity 3D [32] to build a city scene and apply open-source 3D human model library PersonX [39] containing more than 1,000 different persons to generate subjects in the scene. Through the flexible development platform, we can create various scenes to simulate the real world. The cover area is set as $25m \times 25m$, in which all the objects are simulated to the real environment with a scaling.
- Diverse subject settings. To improve the diversity of our dataset. The number of subjects of each frame is different, where the range of subjects in the scene is from 10 to 25, containing 5-20 people walking free and 5 camera wears. Further, we generate every frame by random function, which means camera registration and subject registration are various in each frame.
- Large scale. We create two datasets in our experiments,

- i.e., CSRD-II and CSRD-V. CSRD-II contains two views, while CSRD-V contains five views. In total, CSRD-II includes 2,000 pairs of images, with 1,000 for training and another 1,000 for testing. CSRD-V includes 1,000 groups of images, in which each group contains 5 synchronous images. CSRD-V is only used for testing in our experiments.
- Rich and accurate annotations. Our annotations contain the position (in meters) and face orientation of each subject in the BEV, as well as the camera poses. Besides, we also provide the bounding box with the unified ID number of each subject in all views.

4.2. Setup

Evaluation metrics. To evaluate our proposed method quantitatively, we define the following metrics.

Metric-I: We first evaluate the accuracy of the *camera registration* results, including the position and orientation results in the BEV. For the position, we calculate the distance between the predicted and ground-truth positions. Then we count the average error (*Cam.Pos.Avg*) and the percentages of the error within a list of a certain distance, including 0.5, 1, and 1.5 meters. Similarly, we calculate the angle error in average (*Cam.Ori.Avg*) and percentages of degree errors within certain ranges, including 5, 10 and 15 degrees.

Metric-II: We also evaluate the *subject registration* results. It is similar to the metric-I, which evaluates the position dis-

tance and orientation error of the subjects.

Metric-III: We finally evaluate *cross-view multiple human* association (identification) results. We use precision, recall, and F_1 scores as the metrics.

Comparison methods. As discussed above, there is no method that can directly handle the proposed problem. We include the following comparison methods for the *camera* registration task: DMHA [15] achieves the task of camera registration by using a real BEV image. We provide the FPV image and corresponding BEV image to DMHA. SIFT [27] + KNN [20] and Patch-NetVLAD are two key point matching based methods, which are combined with the classical camera pose estimation method with the matched key points for relative camera estimation. For the second task of subject registration, we include the following two methods. Monoloco++ [6] is a network predict 3D-localization and face orientation of each person in the view. We concatenate it with our proposed geometric transformation and subject fusion methods to evaluate the generalization and validity of our method. MVDet and MVDetr [22, 23] are used for multi-view object detection with the camera calibrations. We provide more details about the implementation details of the comparison methods in the supplementary material.

4.3. Comparative results

Camera Registration Results. We first evaluate the camera registration results on CSRD-II as shown at the top half in Table 1. We can first see that all the comparison methods provide very poor results. Among them, we provide the ground-truth BEV image to DMHA, which is used to find the camera wearer from the BEV instead of our position regression. Both key point matching based methods almost completely fail because of the huge view difference. Monoloco++ generates a relatively acceptable result since it's equipped with the proposed geometric transformation methods. For the proposed method, our mean error of distance is only 0.9 meters, which is less than 1 meters. The most remarkable thing is that our camera angle error within 15 degrees is more than 94%, even within 5 degrees, the percentage is up to 59% and the mean error is less than 6 degrees. This is promising for many real-world applications.

Subject Registration Results. We also evaluate the subject registration in CSRD-II using Metric-II as shown in Table 2. Even MVDet and MVDetr take the camera calibration as prior, our method achieves much superior results in all metrics. At the same time, our method keeps the average distance error within 0.8 meters and the average orientation error within 15 degrees. At the same time, the percentage of angle error within 15 degrees is up to 85.29%, which means our methods can also create accurate subject orientation estimation results in the registered BEV.

Table 3. Cross-view subject association results.

	Precision	Recall	F_1
Baseline [16]	57.48%	82.98%	66.78%
Ours	79.33%	95.45%	85.98%
w GT re-id (oracle)	77.97%	98.18%	86.43%

4.4. Ablation study

We also consider several variations of our method.

- Max/Random: In the candidate camera selection strategy, we choose the max confidence pair or choose randomly instead of our method in Eq. (6).
- w/o pre-train.: Removing the pre-training of LocoNet.
- w/o GT δ_{θ} : Removing the supervision of the camera orientation in Eq. 4.

As shown at the bottom half of Table 1, we can see that no matter whether using the strategy of the max confidence one or the random one, which, not considering the spatialaware selecting strategy, both provide a relatively poor performance than our centroid strategy. The ablation study also verifies the necessity of the pretrained LocoNet. We can also see from the last row that, when removing the camera orientation supervision, the performance only drops a little. This demonstrates that our method is not heavily dependent on the camera orientation supervision, which is not easy to obtain in the real world. We also conduct the ablation study on the subject registration, as shown in Table 2. Similarly to the results above, We can clearly see the effectiveness of the proposed centroid strategy and the pre-trained LocoNet. Also, adding camera orientation labels is helpful to the orientation estimation but not very necessary.

4.5. Cross-view Human Association Results

We further evaluate the results of multi-view human association in CSRD-II, which can verify the effect of the proposed backward self-supervised training strategy. As shown in Table 3, the baseline is the ResNet-50 model pre-trained on the person re-id dataset named Market-1501 [43], on which we apply the self-supervised training strategy as discussed in 3.4. 'w GT re-id' denotes that we provide the ground-truth assignment matrix to supervise the result of the similarity matrix. We can see from Table 3 that our self-supervision strategy improves the F_1 score from the original 66.78% to 85.98% with a large margin. We can also see that our results are very close to the result of supervised training, with only a small gap of 0.45%. The results of the association verify the effectiveness of the proposed self-supervision strategy.

4.6. Multi-view Results

We also evaluate the proposed method on the scenes using multiple cameras for camera and subject registration on CSRD-V, as shown in Table 4.The first row shows the results that we split the 5 views into $C_5^2 = 10$ pair-wise views,

TO 1.1 4 3.6 1.1 1	1 1 1 1 1 1 1 1 1 1 1 1 1 1 1 1 1 1 1 1		
Table / Multi view comercione	d cubiact registration	and multi view cubiec	t accountion reculte
Table 4. Multi-view camera and	д минесттемницации.	and muni-view subject	i association results.

	Cam.Pos.Avg	Cam.Ori.Avg	Cam.Pos.@1	Cam.Ori.@10	Sub.Pos.Avg	Sub.Ori.Avg	Sub.Pos.@1	Sub.Ori.@10	F_1
pair-wise	1.06	6.96	62.71%	79.61%	0.75	14.67	80.76%	58.81%	83.85%
multi-view w/o constraints	1.06	6.93	63.55%	80.60%	1.10	15.64	63.78%	50.47%	85.64%
multi-view w constraints	0.94	6.25	70.84%	84.53%	1.01	15.26	65.02%	50.77%	86.11%

on which we apply the proposed method for two views as above. The second and third rows are the results of multiview subject and camera registration without or with the constraints during subject matching in Section 3.3. We can see that using the proposed constraints will effectively improve the results on both camera registration, subject registration and multi-view subject association. Compared with the results of two views registration, we can see that even though the results are slightly worse in 5 views, the overall results are still very good, which demonstrates the stability of our method in multiple views.

4.7. Visualization

We show several qualitative results. Figure 7 shows the successful cases, in which we can see that the prediction of both camera and subject registration can achieve a good coincidence with the ground truth, thanks to the high accuracy of our method. We specifically picked a case with errors to illustrate some limitations of our method in Figure 8. The first problem comes from the subject association module. Given the cross-view subject association errors, there may be some incorrect matches, which lead to the wrong fusions. The second one is that the screen may have very serious occlusion, someone may be occluded in the crowd, which can not be seen in all FPVs.

We also provide the real-world case, as shown in Figure 9. Note that, we directly apply our method to the real world case without any additional annotation. We can see that, except for a wrong fusion coming from the incorrect matching, the prediction of the subject and camera distributions are very close to the real BEV. This demonstrates the robustness and generalization of the proposed method.

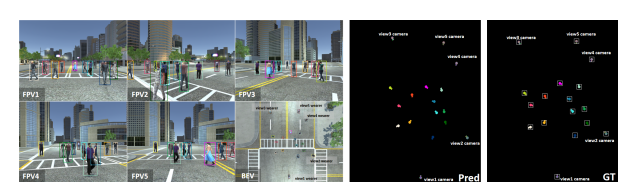


Figure 7. Qualitative case analysis. To distinguish the prediction one and the ground truth one, we add a white rectangle around every ground-truth subject.

5. Discussion

Limitation. 1) The main experiments in this work are conducted on the synthetic dataset. In the future, we plan to test and improve the proposed method on more real-world



Figure 8. Failure case analysis.



Figure 9. Real-world case study.

cases by collecting some new data. 2) Our geometric transformation only uses the aligned pair from pedestrians. In the future, we hope to expand our methods that can use the aligned points from any objects, not only pedestrians.

Applications. The setting of our work is a multi-view scenario with mobile cameras, which is very common in the real world. They are appropriate for outdoor scenes without a fixed camera installed. For practical application scenarios, especially in outdoor video surveillance, e.g., important person detection [19], interaction/group activity recognition and analysis [42], the mobile cameras are practical. However, it is very hard to apply the calibration based method. In this case, the proposed method is useful, which only needs the multi-view RGB images as input and provides promising results.

6. Conclusion

In this paper, we have studied a new problem of multiview cameras and subject registration in BEV without camera calibrations. For this problem, we developed a new approach that can simultaneously handle two tasks – camera registration, subject registration. Specifically, the proposed method uses an end-to-end framework, which makes full use of deep network based appearance information and multiple view geometry based spatial knowledge to handle the above tasks effectively. We also create a new synthetic dataset with various settings and rich annotations. Experimental results show the superior performance of our methods. In the future, we plan to extend our approach to scenarios where the subjects are not limited to just pedestrians.

References

- Shervin Ardeshir and Ali Borji. Ego2top: Matching viewers in egocentric and top-view videos. In *Proceedings of the European Conference on Computer Vision*, pages 253–268, 2016.
- [2] Shervin Ardeshir and Ali Borji. Egocentric meets top-view. IEEE Transactions on Pattern Analysis and Machine Intelligence, 41(6):1353–1366, 2018. 3
- [3] Shervin Ardeshir and Ali Borji. Integrating egocentric videos in top-view surveillance videos: Joint identification and temporal alignment. In *Proceedings of the European Conference on Computer Vision*, pages 285–300, 2018. 3
- [4] Pierre Baqué, François Fleuret, and Pascal Fua. Deep occlusion reasoning for multi-camera multi-target detection. In *Proceedings of the IEEE International Conference on Computer Vision*, pages 271–279, 2017. 1, 2
- [5] Lorenzo Bertoni, Sven Kreiss, and Alexandre Alahi. Monoloco: Monocular 3d pedestrian localization and uncertainty estimation. In *Proceedings of the IEEE/CVF International Conference on Computer Vision*, pages 6861–6871, 2019.
- [6] Lorenzo Bertoni, Sven Kreiss, and Alexandre Alahi. Perceiving humans: from monocular 3d localization to social distancing. *IEEE Transactions on Intelligent Transportation* Systems, 2021. 2, 6, 7
- [7] Tolga Birdal, Emrah Bala, Tolga Eren, and Slobodan Ilic. Online inspection of 3d parts via a locally overlapping camera network. In *Proceedings of the IEEE Winter Conference on Applications of Computer Vision*, pages 1–10. IEEE, 2016. 2
- [8] Andrea Censi, Antonio Franchi, Luca Marchionni, and Giuseppe Oriolo. Simultaneous calibration of odometry and sensor parameters for mobile robots. *IEEE Transactions on Robotics*, 29(2):475–492, 2013.
- [9] Tatjana Chavdarova, Pierre Baqué, Stéphane Bouquet, Andrii Maksai, Cijo Jose, Timur Bagautdinov, Louis Lettry, Pascal Fua, Luc Van Gool, and François Fleuret. Wildtrack: A multi-camera hd dataset for dense unscripted pedestrian detection. In *Proceedings of the IEEE Conference on Computer Vision and Pattern Recognition*, pages 5030–5039, 2018.
- [10] Tatjana Chavdarova and François Fleuret. Deep multicamera people detection. In *Proceedings of the IEEE International Conference on Machine Learning and Applications*, pages 848–853, 2017. 1, 2
- [11] Hansheng Chen, Yuyao Huang, Wei Tian, Zhong Gao, and Lu Xiong. Monorun: Monocular 3d object detection by reconstruction and uncertainty propagation. In *Proceedings of the IEEE/CVF Conference on Computer Vision and Pattern Recognition*, pages 10379–10388, 2021. 1, 2
- [12] Junting Dong, Qi Fang, Wen Jiang, Yurou Yang, Qixing Huang, Hujun Bao, and Xiaowei Zhou. Fast and robust multi-person 3d pose estimation and tracking from multiple views. *IEEE Transactions on Pattern Analysis and Machine Intelligence*, 2021. 2
- [13] Shuai Dong, Xinxing Shao, Xin Kang, Fujun Yang, and Xiaoyuan He. Extrinsic calibration of a non-overlapping cam-

- era network based on close-range photogrammetry. *Applied optics*, 55(23):6363–6370, 2016. 2
- [14] Ruize Han, Wei Feng, Yujun Zhang, Jiewen Zhao, and Song Wang. Multiple human association and tracking from egocentric and complementary top views. *IEEE Transactions on Pattern Analysis and Machine Intelligence*, 2021. 1, 2
- [15] Ruize Han, Yiyang Gan, Jiacheng Li, Feifan Wang, Wei Feng, and Song Wang. Connecting the complementary-view videos: Joint camera identification and subject association. In *Proceedings of the IEEE/CVF Conference on Computer Vision and Pattern Recognition*, pages 2416–2425, 2022. 1, 2, 6, 7
- [16] Ruize Han, Yun Wang, Haomin Yan, Wei Feng, and Song Wang. Multi-view multi-human association with deep assignment network. *IEEE Transactions on Image Processing*, 31:1830–1840, 2022. 5, 7
- [17] Ruize Han, Yujun Zhang, Wei Feng, Chenxing Gong, Xiaoyu Zhang, Jiewen Zhao, Liang Wan, and Song Wang. Multiple human association between top and horizontal views by matching subjects' spatial distributions. *arXiv preprint arXiv:1907.11458*, 2019. 1, 2
- [18] Ruize Han, Jiewen Zhao, Wei Feng, Yiyang Gan, Liang Wan, and Song Wang. Complementary-view co-interest person detection. In *Proceedings of the ACM International Conference on Multimedia*, pages 2746–2754, 2020. 1, 2
- [19] Ruize Han, Jiewen Zhao, Wei Feng, Yiyang Gan, Liang Wan, and Song Wang. Complementary-view co-interest person detection. In *Proceedings of the ACM International Conference* on Multimedia, 2020. 8
- [20] Stephen Hausler, Sourav Garg, Ming Xu, Michael Milford, and Tobias Fischer. Patch-netvlad: Multi-scale fusion of locally-global descriptors for place recognition. In *Proceedings of the IEEE/CVF Conference on Computer Vision and Pattern Recognition*, pages 14141–14152, 2021. 2, 6, 7
- [21] Jun Hayakawa and Behzad Dariush. Recognition and 3d localization of pedestrian actions from monocular video. In Proceedings of the IEEE International Conference on Intelligent Transportation Systems, pages 1–7, 2020. 2
- [22] Yunzhong Hou and Liang Zheng. Multiview detection with shadow transformer (and view-coherent data augmentation). In *Proceedings of the ACM International Conference on Multimedia*, pages 1673–1682, 2021. 1, 2, 6, 7
- [23] Yunzhong Hou, Liang Zheng, and Stephen Gould. Multiview detection with feature perspective transformation. In *Proceedings of the European Conference on Computer Vision*, pages 1–18, 2020. 1, 2, 6, 7
- [24] Qi-Xing Huang and Leonidas Guibas. Consistent shape maps via semidefinite programming. In *Computer graphics* forum, volume 32, pages 177–186, 2013. 5
- [25] S. Kreiss, L. Bertoni, and A. Alahi. Pifpaf: Composite fields for human pose estimation. In arXiv, 2019. 3
- [26] Zhen Liu, Fengjiao Li, and Guangjun Zhang. An external parameter calibration method for multiple cameras based on laser rangefinder. *Measurement*, 47:954–962, 2014. 2
- [27] David G Lowe. Distinctive image features from scaleinvariant keypoints. *International journal of computer vi*sion, 60(2):91–110, 2004. 6, 7

- [28] Shujie Luo, Hang Dai, Ling Shao, and Yong Ding. M3dssd: Monocular 3d single stage object detector. In *Proceedings of the IEEE/CVF Conference on Computer Vision and Pattern Recognition*, pages 6145–6154, 2021. 1, 2
- [29] Xinzhu Ma, Yinmin Zhang, Dan Xu, Dongzhan Zhou, Shuai Yi, Haojie Li, and Wanli Ouyang. Delving into localization errors for monocular 3d object detection. In *Proceedings of the IEEE/CVF Conference on Computer Vision and Pattern Recognition*, pages 4721–4730, 2021. 1, 2
- [30] Robert Clay Prim. Shortest connection networks and some generalizations. The Bell System Technical Journal, 36(6):1389–1401, 1957. 5
- [31] Cody Reading, Ali Harakeh, Julia Chae, and Steven L Waslander. Categorical depth distribution network for monocular 3d object detection. In *Proceedings of the IEEE/CVF Conference on Computer Vision and Pattern Recognition*, pages 8555–8564, 2021. 1
- [32] John Riccitiello. John riccitiello sets out to identify the engine of growth for unity technologies (interview). *VentureBeat. Interview with Dean Takahashi. Retrieved January*, 18(3), 2015. 6
- [33] Paul-Edouard Sarlin, Daniel DeTone, Tomasz Malisiewicz, and Andrew Rabinovich. Superglue: Learning feature matching with graph neural networks. In *Proceedings of the IEEE/CVF Conference on Computer Vision and Pattern Recognition*, pages 4938–4947, 2020. 2
- [34] Johannes L Schonberger and Jan-Michael Frahm. Structurefrom-motion revisited. In *Proceedings of the IEEE Con*ference on Computer Vision and Pattern Recognition, pages 4104–4113, 2016. 2
- [35] Matthew Shere, Hansung Kim, and Adrian Hilton. 3d human pose estimation from multi person stereo 360 scenes. In *CVPR Workshops*, pages 1–8, 2019. 2
- [36] Yujiao Shi, Liu Liu, Xin Yu, and Hongdong Li. Spatial-aware feature aggregation for image based cross-view geolocalization. *Advances in Neural Information Processing Systems*, 32, 2019. 2
- [37] Yujiao Shi, Xin Yu, Dylan Campbell, and Hongdong Li. Where am i looking at? joint location and orientation estimation by cross-view matching. In *Proceedings of the IEEE/CVF Conference on Computer Vision and Pattern Recognition*, pages 4064–4072, 2020. 2
- [38] Liangchen Song, Jialian Wu, Ming Yang, Qian Zhang, Yuan Li, and Junsong Yuan. Stacked homography transformations for multi-view pedestrian detection. In *Proceedings of the IEEE/CVF International Conference on Computer Vision*, pages 6049–6057, 2021. 1, 2
- [39] Xiaoxiao Sun and Liang Zheng. Dissecting person reidentification from the viewpoint of viewpoint. In Proceedings of the IEEE/CVF Conference on Computer Vision and Pattern Recognition, 2020. 6
- [40] Xiao Tan, Zhigang Wang, Minyue Jiang, Xipeng Yang, Jian Wang, Yuan Gao, Xiangbo Su, Xiaoqing Ye, Yuchen Yuan, Dongliang He, et al. Multi-camera vehicle tracking and reidentification based on visual and spatial-temporal features. In CVPR Workshops, pages 275–284, 2019. 2

- [41] Li Wang, Liang Du, Xiaoqing Ye, Yanwei Fu, Guodong Guo, Xiangyang Xue, Jianfeng Feng, and Li Zhang. Depthconditioned dynamic message propagation for monocular 3d object detection. In Proceedings of the IEEE/CVF Conference on Computer Vision and Pattern Recognition, pages 454–463, 2021. 1, 2
- [42] Jiewen Zhao, Ruize Han, Yiyang Gan, Liang Wan, Wei Feng, and Song Wang. Human identification and interaction detection in cross-view multi-person videos with wearable cameras. In *Proceedings of the ACM International Conference* on Multimedia, 2020. 8
- [43] Liang Zheng, Liyue Shen, Lu Tian, Shengjin Wang, Jingdong Wang, and Qi Tian. Scalable person re-identification: A benchmark. In *Proceedings of the IEEE International Conference on Computer Vision*, pages 1116–1124, 2015. 7